17th World Conference on Earthquake Engineering, 17WCEE
Sendai, Japan - September 13th to 18th 2020

LOCATING DAMAGE TO BUILDINGS USING A DISPLACEMENT FREQUENCY RESPONSE FUNCTION-BASED APPROACH

S. L. Hung[(1)], X. Z. Chen[(2)], C. Y. Kao[(3)]

(1) Professor, Department of Civil Engineering, National Chiao Tung University, slhung@mail.nctu.edu.tw
(2) Graduate Student, Department of Civil Engineering, National Chiao Tung University, jacky201.tw@yahoo.com.tw
(3) Associate Professor, Department of Applied Geoinformatics, Chia Nan University of Pharmacy & Science, chingyun@mail.cnu.edu.tw

Abstract

Vibration-based structural damage detection approach is the in-situ nondestructive sensing and analysis of the characteristics of a structure, including the structural response to external excitations, for the purpose of detecting changes that may indicate damage or degradation of materials. The feasibility of applying various vibration characteristics, such as natural frequencies, mode shapes, mode shape curvatures, modal flexibility, and frequency response functions, to damage identification of structures has received considerable attention in the past few decades. Frequency response function (FRF) data can provide much more information on damage in a desired frequency range compared to modal data that is extracted from a very limited range around resonances. Among structural health monitoring techniques FRF-based methods have the potential to locate structural damage of building structures. Conventional structural damage detection technology collects structural response data by using contact systems, such as displacement or acceleration transducers. However, installing these contact systems can be expensive in cost, time, and labor. To overcome these difficulties, several non-contact measurement technologies, such as optical, laser, radar, or GPS, have also been developed. Given the rapid advances in optical imaging hardware technology, the use of digital photography in structural monitoring systems has attracted considerable attention. This work presents a displacement FRF-based approach for locating damage to building structures which enhance the work of Lin et al. (2012). Furthermore, the feasibility of applying the proposed approach to locate damage to building structures using displacement measured by a digital camera combined with digital image correlation techniques is also investigated in this study. A numerical example and an experimental example are presented to demonstrate the feasibility of using the proposed approach to locate damage to building structures for signal and multiple nonadjacent damage locations.

Keywords: structural health monitoring, frequency response function, digital image correlation, locating damage

1. Introduction

Damage detection of structures via vibration-based measurement approaches is the in-situ nondestructive sensing and analysis of the characteristics of a structure, for the purpose of detecting changes that may indicate damage or degradation of structures. The feasibility of applying various vibration characteristics, such as natural frequencies, mode shapes, mode shape curvatures, modal flexibility, and frequency response functions, to damage identification of structures, has received considerable attention in the past few decades [1-2].

Some research has shown that FRF-based methods are highly promising approaches to detect damage to building structures [3-7]. Ni et al. [3] detected the seismic damage of a 38-story tall building using measured FRFs and neural networks. Their study used principal component analysis (PCA) to reduce dimension and eliminate noise of measured FRFs. The PCA-compressed FRF data are then used as input to neural networks for damage identification. Furukawa et al. [4] developed an approach to detect damage to building structures that uses uncertain FRFs based on a statistical bootstrap method. Kanwar et al. [5] identified damage of reinforced concrete buildings using FRFs. Hsu and Loh [6] detected damage of building structure subjected to earthquake ground excitation using FRFs of intact and damaged systems as well as system matrices of the intact system to derive the damage identification equations. Lin et al. [7] proposed a substructure-based FRF approach that uses index, *SubFRFDI*, to locate damage to building structures. Lee and Shin [8] specified two main advantages of using the frequency response function (FRF) data for structural damage detection. Firstly, modal data can be contaminated by modal extraction errors in addition to measurement errors, due to they are derived data sets. Secondly, a complete set of modal data cannot be measured in all but the simplest structures. FRF data can provide much more information on damage in the desired frequency range compared to modal data that is extracted from a very limited range around resonances.

Along with data analysis approaches, data measurement is another issue that needs to be solved for detecting damage to structures. Contact systems are the major conventional structural damage detection technology for collecting structural response data, such as displacement or acceleration transducers. However, installing these contact systems can be expensive in labor, cost, and time [9]. To overcome these obstacles, some non-contact measurement technologies have also been developed, such as optical, laser, radar, and GPS [10]. Given the rapid advances in optical imaging hardware technology, the use of digital photography in structural monitoring systems has attracted considerable attention. Digital image correlation (DIC) is a measurement technique which extends the principles of photogrammetry to obtain full-field surface displacement measurements of an object using digital cameras. Several researchers applied DIC to detect damage of building structures using dynamic responses [11-16]. Shih et al. [11-12] developed a low-cost digital image correlation method to measure dynamic response of shear buildings. The accuracy of the DIC method is sufficiently high for several applications. Combe and Richefeu [13] used DIC technique coupled with geometrical rules to develop an approach to track nonsmooth trajectory of particles. Sieffert et al. [14] presented a digital correlation technique to capture the full-field displacement by using a high-speed camera of a full scale structure tested on a shaking table. Lu et al. [15] presented a digital image processing approach with a unique hive triangle pattern by integrating subpixel analysis for noncontact measurement of structural dynamic response data. To save computation time of this approach, Hung and Lu [16] integrated this approach and GPU computing technique.

The aim of this work is to enhance the work of Lin et al. [7]. A damage location index (*CurveFRFDI)* based on *SubFRFDI* curvature is employed to locate damage of building structures in this work to enhance the sensitivity of *SubFRFDI* to damage detection. Additionally, this work aims to investigate the feasibility of applying the proposed approach to locate damage to building structures using displacement measured by digital camera combined with DIC technique. Moreover, a numerical example and an experimental example demonstrate the feasibility of applying the proposed approach for locating damage to building structures.

2. Strategy of Damage Location

Lin et al. [7] presented a substructure-based FRF approach to locate damage to shear-typed building structures. As presented in Fig. 1, the ith substructure is a structure contains the ith –Nth floors (or degree of freedoms, DOFs) for an N-story building structure. Since this work investigates the feasibility of applying displacement measured by digital camera combined with DIC technique to locate damage to building structures, the substructure-based FRFs of the jth DOF in the ith substructure is then modified as

$$\tilde{H}_j^{(i)}(\omega) = \frac{\tilde{X}_j}{\tilde{X}_{i-1}}, \quad j = i \; to \; N \tag{1}$$

where $\tilde{X}_j$ and $\tilde{X}_{i-1}$ are the Fourier transforms of $\tilde{x}_j(t)$ and $\tilde{x}_{i-1}(t)$, respectively; $\tilde{x}_j(t)$ and $\tilde{x}_{i-1}(t)$ are the absolute displacement of the j^{th} and $(i\text{-}1)^{th}$ DOF, respectively. Notionally, when the damage is assumed to have occurred in the column(s) between the i^{th} and $(i\text{-}1)^{th}$ DOFs, the substructure-based FRF is significantly altered in the i^{th} DOF, as described by $\tilde{H}_i^{(i)}(\omega)$. For efficiency, only one substructure-based FRF, $\tilde{H}_i^{(i)}(\omega)$, is determined for each substructure to reduce the computational time and damage is located based on the FRFs, $\tilde{H}_1^{(1)}(\omega)$, $\tilde{H}_2^{(2)}(\omega)$, $\cdots$, $\tilde{H}_N^{(N)}(\omega)$, of all substructures.

The *SubFRFDI*, index of substructure-based FRF damage location, for the i^{th} substructure is defined as

$$SubFRFDI_i = 1 - Exp\left[-\rho^2\left(\sum_{\omega=a}^{b}\left\{\left(NDF_i(\omega)\right)^2\right\}\right)/n\right] \tag{2}$$

where ρ, a, b, and n are working parameters and the $\mathrm{NDF_i}(\omega)$ is expressed as

$$NDF_i(\omega) = \frac{\bar{P}_i(\omega)}{max\left[\left|\tilde{H}_{i,d}^{(i)}(\omega)\right|_{max}, \left|\tilde{H}_{i,u}^{(i)}(\omega)\right|_{max}\right]} \tag{3}$$

and the absolute dissimilarity $\bar{P}_i(\omega)$ is defined as

$$\bar{P}_i(\omega) = \left|\left|\tilde{H}_{i,d}^{(i)}(\omega)\right| - \left|\tilde{H}_{i,u}^{(i)}(\omega)\right|\right| \tag{4}$$

where $\left|\tilde{H}_{i,d}^{(i)}(\omega)\right|$ and $\left|\tilde{H}_{i,u}^{(i)}(\omega)\right|$ are the magnitudes of $\tilde{H}_i^{(i)}$ in the damaged and undamaged states, respectively. These N dissimilarities, $\bar{P}_1(\omega)\sim\bar{P}_N(\omega)$, can be correspondingly computed for a shear building with N floors. In Eq. (2), the coefficient ρ is a control between 0 and 1. The range of selected frequencies for calculating *SubFRFDI* is set to be a~b, where a is a starting frequency of zero and b is the end frequency, which equals the first modal frequency (undamaged state). The coefficients a and b are determined by trial-and-error process. The value n equals (b-a) divided by sampling time. If the properties of a structural system do not change, then $SubFRFDI_i$ is close to zero. However, if the damage to i^{th} floor in a shear building is severe, then the value of $SubFRFDI_i$ is high. Thus $SubFRFDI_i$ can be regarded as the *SubFRFDI* corresponding to location i (the i^{th} floor).

It revealed in the previous work [7], with the increasing of damage extent, the *SubFRFDI* values corresponding to damaged and undamaged locations increase. Consequently *SubFRFDI* is insensitive to damage with larger damage extent. Moreover, *SubFRFDI* is able to locate single and multiple nonadjacent damages, but it is unable to locate multiple nonadjacent damages to building structures. A damage location index (*CurveFRFDI)* based on *SubFRFDI* curvature can enhance the sensitivity of *SubFRFDI* to locate damage to building structures. The curvature of $SubFRFDI_i$, $K(SubFRFDI_i)$, can be simply defined as follows

$$K(SubFRFDI_i) = SubFRFDI_{i+1} + SubFRFDI_{i-1} - 2SubFRFDI_i \;\; \text{for } i=1, 2, \ldots, N \tag{5}$$

where $SubFRFDI_0$ and $SubFRFDI_{N+1}$ are both equal to zero. To enhance the sensitivity of *SubFRFDI* to single and nonadjacent damage, a damage location index based on *SubFRFDI* curvature, *CurveFRFDI*, is employed to locate damage to building structures in this work. The *CurveFRFDI* is expressed as follows for an *N*-story building structure

$$CurveFRFDI_i = \begin{cases} -K(SubFRFDI_i) & if\ K(SubFRFDI_i) < 0 \\ \frac{K(SubFRFDI_i)}{A} & if\ K(SubFRFDI_i) \geq 0 \end{cases} \quad (6)$$

where *A* is a control value that scales $CurveFRFDI_i$ to a very small positive value for positive $SubFRFDI_i$ curvature. Compared with *SubFRFDI* curvature, the value of coefficient *A* is large, and *A* is set to be 100 in this work. The range of $CurveFRFDI_i$ is from 0 to infinite. Similar to *SubFRFDI*, damage occurred at the location corresponding to a larger value of *CurveFRFDI*.

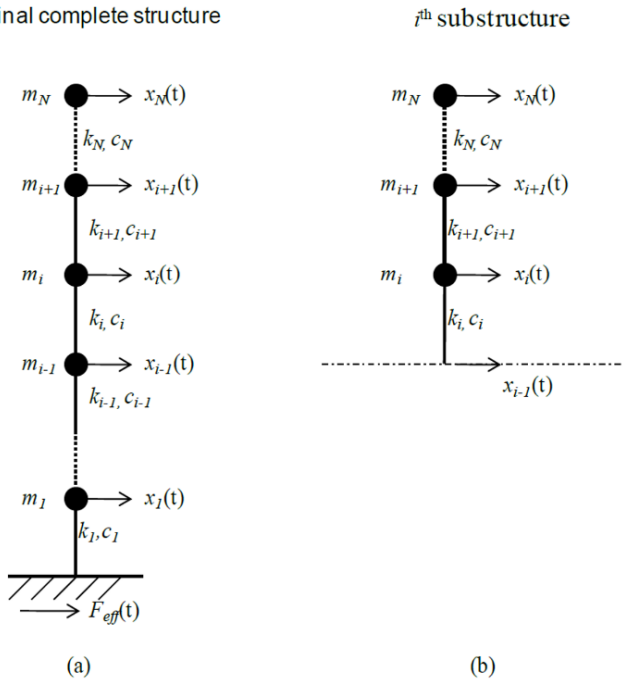

Fig. 1 – (a) Original complete structure, (b) the *i*th substructure "(Fig. 1 is reproduced from Lin et al., 2012), (under the Creative Commons Attribution License/public domain)"

3. Digital Image Correlation

Digital Image Correlation (DIC) is an optical technique to measure continuous deformation by tracking the position of the same physical points shown in a reference image and a corresponding deformed image. This work employs the DIC approach presented in the work of Lu et al. [15] for displacement measurement in the experimental example. The approach used a unique hive triangle pattern by integrating subpixel analysis for noncontact measurement of structural dynamic response data.

As shown in Fig. 2(b) and 2(c), a fixed-size rectangular subset of pixels that cover hive triangle patterns is the region of interest (ROI), contained both within the reference (source) and within the deformed (target) images and marked as a red color box. Meanwhile, in Fig. 2(a), the source and target images are designated as *I* and *I*', respectively. The (x_0, y_0) and (x_1, y_1) are the coordinates of the points at the left-top of the ROI of the

source image and the after deformed target images respectively. Hence, u and v are the relative deformations of a particular point in image space. The coordinates of (x_0, y_0) and (x_1, y_1) are figured out in the following steps. Two images are first selected as S and T. The image S is an undeformed (source) image, and image T is a slightly deformed image (target) relative to image S. The difference between the two images, S and T, can be estimated through a simple difference method via pixel-wise computation. If the intensity of each pixel is from 0 to 255, the difference of each pixel between S and T is maximal as the equation value is 255, and S and T are exactly identical when the equation value is 0. If two images have the same background, the difference of the pixels in the background area close to zero. Therefore, if an ROI changes the position due to deformation, the difference these pixels covered in the ROI is relatively large.

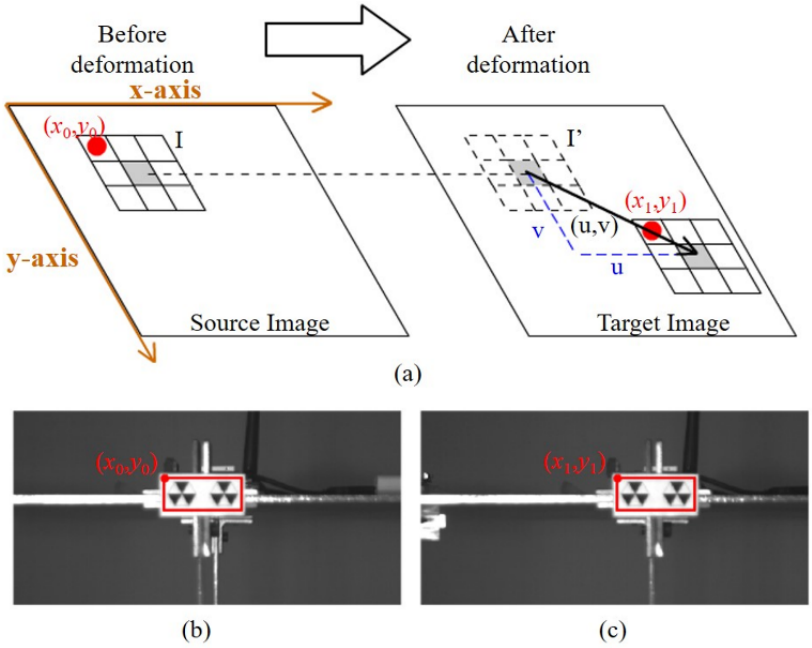

Fig. 2 – (a) Simplified diagram of source and target image, showing displacement variation of image block. (b) Source image. (c) Target image. "Fig. 2 is reproduced from Lu et al. [15] (under the Creative Commons Attribution License/public domain)"

Moreover, the coordinate, (x_0, y_0), of the ROI of the source image can be computed using a mean-max method. The method first calculates the means of the intensities of all columns and rows pixels in the source and one of the target images having slightly deformation. Particularly, the approach of Lu et al. employs an ideal hive triangle pattern as the ROI in calculating the correlation coefficient with the source image. The correlation coefficient used in the work is defined in the following equation:

$$CC = \frac{\sum\sum[(f-\langle f\rangle)\cdot(g-\langle g\rangle)]}{\{\sum\sum(f-\langle f\rangle)^2\cdot\sum\sum(g-\langle g\rangle)^2\}^{1/2}} \tag{7}$$

where f and g are the pixel value of ROIs for the source and target images, respectively. The sign $\langle\cdot\rangle$ denotes the mean operator and $\langle f\rangle$ and $\langle g\rangle$ are the means of ROIs in the source and target images, respectively. The coordinate, (x_1, y_1), of the point at the left-top of the ROI of the after deformed target images can be figured out based on the following equation.

$$(x_1, y_1) = max[CC\ (I_{x_0,y_0}, I'_{x_1,y_1})] \tag{8}$$

where I and I' denote the aforementioned ROIs for source and target images, and CC refers to the correlation coefficient function to evaluate with the two ROIs. The relative displacement, (d_x, d_y), in the unit pixels can be estimated to be $(x_1\text{-}x_0, y_1\text{-}y_0)$ in the x-axis and y-axis coordinates and the precision of the displacement, is an integer pixel value. If the actual length (L) of the pattern is a known quantity, and the pixel width (W) of the pattern has been evaluated by the measurement system, then the actual displacement, (u, v), can be calculated by using estimated pixel displacement, (d_x, d_y), to multiply by a pixel ratio (R_p), equal to L/W.

The subpixel analysis can improve the precision based on the subpixel estimation of a target image. The results of Lu et al. [15] indicated that the measurement system increases the precision to a pixel value of 0.1, or even 0.01, and the precision achieves 0.01mm if R_p is less than 0.1mm. By employing a non-contacted approach for measurement of structural dynamic response data, the record can be divided into 9,000 image frames if the time history of displacements is recorded as a video that contains 90 seconds with 100 fps data. The first frame will be set as a source (reference) image, and other frames are the target images and are processed sequentially to obtain the coordinates (x_1, y_1) in each target image; consequently, the time history of displacements can be figured out.

4. Examples

To ratify the practicability of the proposed approach for locating damage to building structures, a numerical example and an experimental example are studied in this work.

4.1 Numerical Example

A six-story shear plane frame structure, each floor with the same structural parameters, is studied to assess the feasibility of the proposed approach for locating damage. In this example, the damage is simulated as reduced floor stiffness. 43 simulated cases, including 15 single damage location and 28 multiple damage locations, are studied in this work. 1995 Kobe earthquake record is used as the external excitation, but normalized to 100 gal as the Peak Ground Acceleration (PGA).

Figs. 3 and 4 show that *SubFRFDI* values corresponding to damaged and undamaged locations increase with the increase in damage extent for cases of single and multiple damage locations. Thus, false detection could occur for large damage extent cases if the number of damage location is unknown. For cases of multiple nonadjacent damage locations, Dam_2F&4F15% (Fig. 4(a)) and Dam_2F&4F&6F15% (Fig. 4(b)), the damage locations can be predicted by the location (the lowest floor of the substructure) corresponding to the local maximum value of *SubFRFDI*. However, this criterion is not suitable for cases of multiple adjacent damage locations such as cases Dam_2F&3F15% and Dam_2F&3F&4F15%.

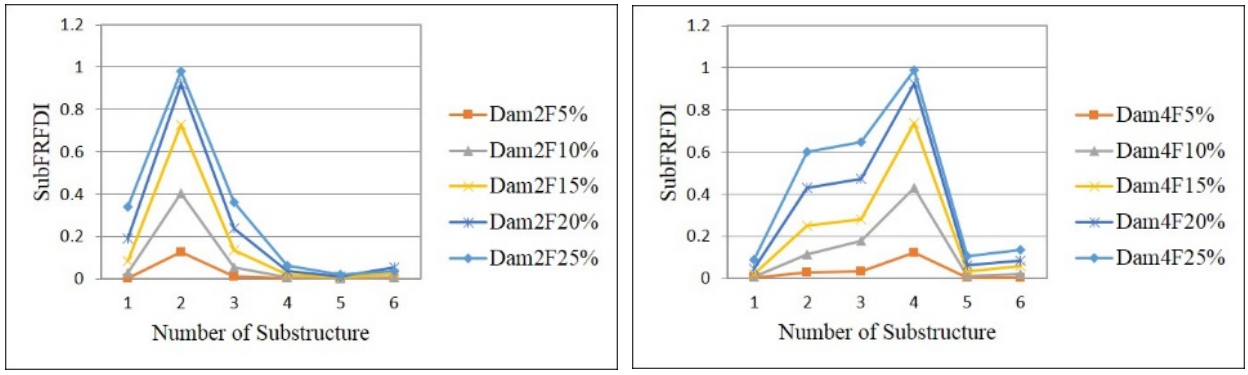

(a) (b)

Fig. 3 – The comparison of the *SubFRFDI* for 5%, 10%, 15%, 20%, and 25% stiffness reduction in (a) the 2nd floor (b) the 4th floor

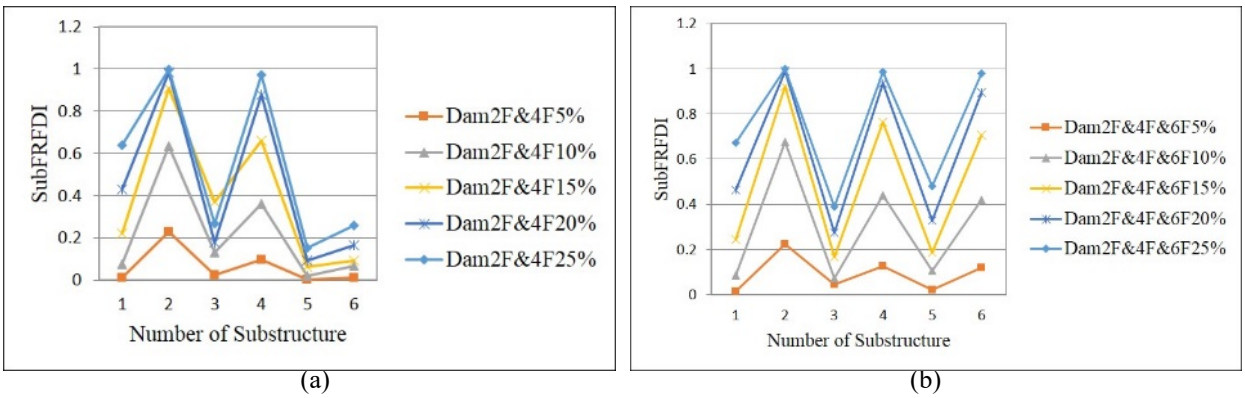

(a) (b)

Fig. 4 –The comparison of the *SubFRFDI* for 5%, 10%, 15%, 20%, and 25% stiffness reduction in (a) the 2nd and the 4th floors (b) the 2nd, the 4th, and the 6th floors

For cases of damage location using *CurveFRFDI*, Fig. 5 shows the comparison between *SubFRFDI* and *CurveFRFDI* for a single damage location. The comparison results indicates that *CurveFRFD*I is more precise than *CurveFRFD*I. Figs. 6 and 7 show that *CurveFRFDI* values corresponding to damaged and undamaged locations increase with the increase in damage extent for cases of single and multiple damage locations. Results show that *CurveFRFDI* has higher sensitivity to damage than *SubFRFDI* for cases of single and multiple damage locations as compared Figs. 6-7 with Figs. 3-4. Mowever, results also imply that *CurveFRFDI* is unable to locate damage for cases of multiple adjacent damage locations. For example, the 3rd floor for case Dam_2F&3F15% and the 3rd floor for case Dam_2F&3F&4F15% (see Fig. 8(a) and (b)) are falsely detected. For most cases, the *CurveFRFDI* value corresponding to the damaged location increases with the increase in damage extent while that corresponding to the undamaged location is almost zero and varies slightly with the increase in damage extent. It indicates that *CurveFRFDI* can locate damage regardless of intensity (extent) for most cases. Notably, detecting small extent damage is an important issue for early warning of structural health monitoring.

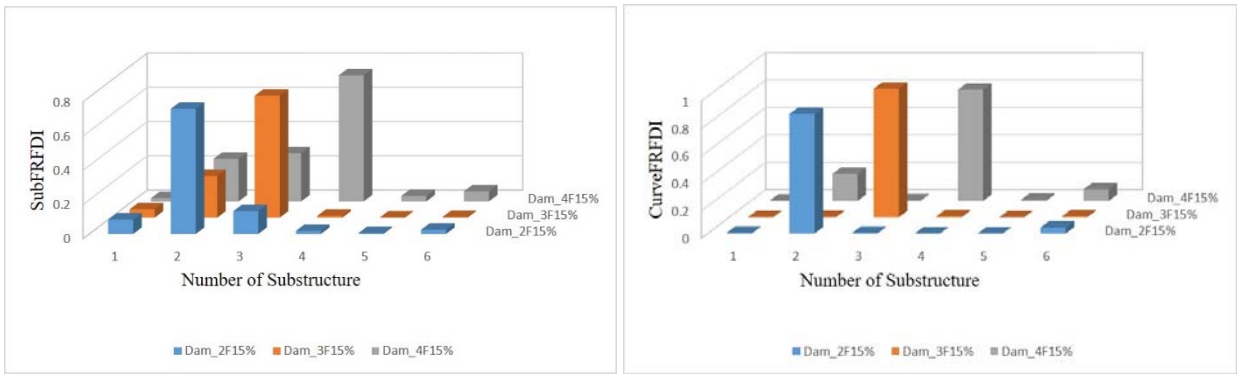

(a) (b)

Fig. 5 – The comparison of the *SubFRFDI* and *CurveFRFDI* values for single damage cases (Dam_2F15%, Dam_3F15%, and Dam_4F15%)

4.2 Experimental Example

A 1/3 scale eight-story steel frame (Fig. 9), subjected to the Chi-Chi earthquake for different values of PGA (50 gal, 100 gal, 200gal, 500 gal, and 1200gal) shaking table tests, are processed to demonstrate the feasibility of the proposed approach for locating damage. This series shaking table tests were undertaken by The National Center for Research on Earthquake Engineering (NCREE) in Taiwan. The displacements response histories of

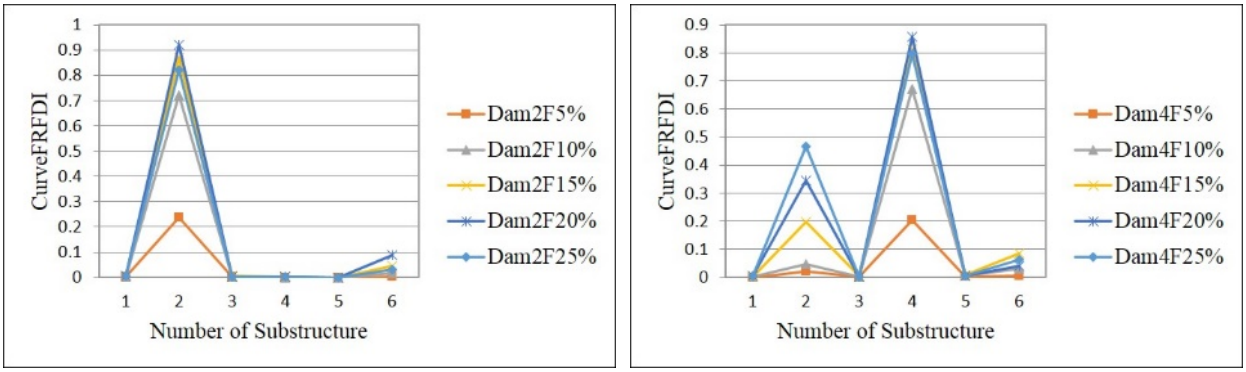

(a) (b)

Fig. 6 – The comparison of the CurveFRFDI for 5%, 10%, 15%, 20%, and 25% stiffness reduction in (a) the 2nd floor (b) the 4th floor

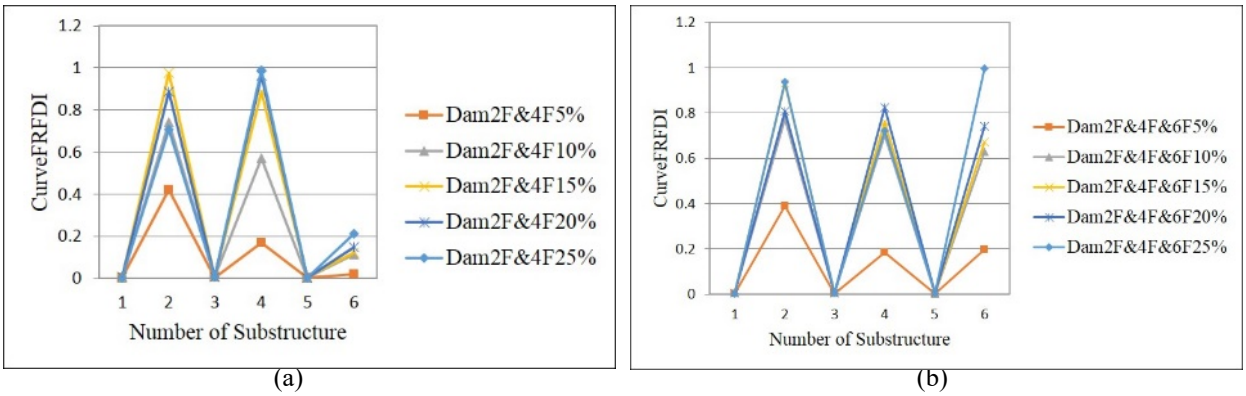

(a) (b)

Fig. 7 –The comparison of the *CurveFRFDI* for 5%, 10%, 15%, 20%, and 25% stiffness reduction in (a) the 2nd and the 4th floors (b) the 2nd, the 4th, and the 6th floors

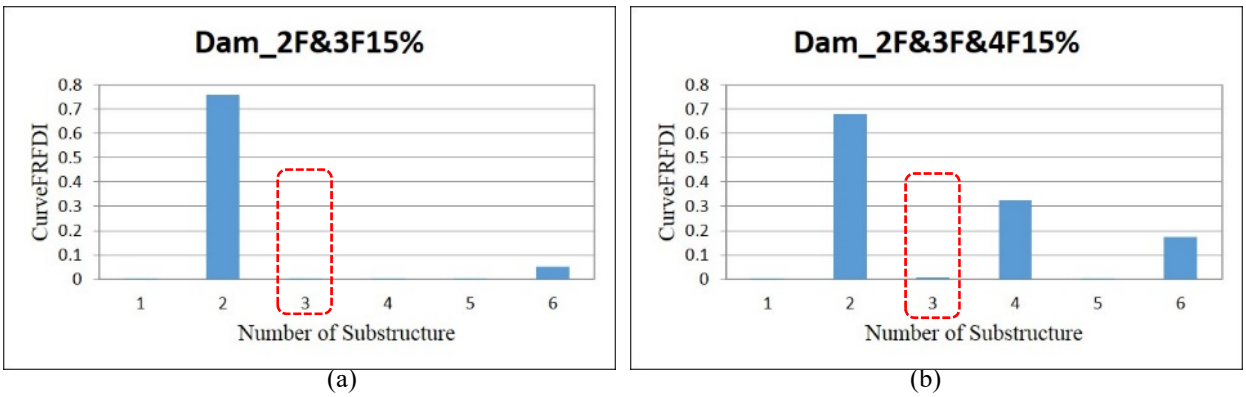

(a) (b)

Fig. 8 – *CurveFRFDI* values for (a) case Dam_2F&3F15% (b) case Dam_2F&3F&4F15%

each floor are measured during the shaking table tests by linear variation differential transformation (LVDT) and a digital camera (Basler A504kc, sampling rate of 500Hz) combined with the DIC approach presented in the work of Lu et al. [15], abbreviated as LVDT-measured data and DIC-measured data following The damage in this example is simulated by reducing the cross-section of certain columns. Single and multiple nonadjacent damage locations are both investigated. Table 1 presents the simulated damage cases.

Fig. 9 –The eight-story steel frame

Table 1. Damage scenarios of the experimental example

Case	Damage Location	External Excitation
Dam50_1F	the 1st floor	The Chi-Chi earthquake with PGA=50 gal
Dam100_1F	the 1st floor	The Chi-Chi earthquake with PGA=100gal
Dam50_1F&3F	the 1st and the 3rd floors	The Chi-Chi earthquake with PGA=50 gal
Dam100_1F&3F	the 1st and the 3rd floors	The Chi-Chi earthquake with PGA=100gal
Dam200_1F&3F	the 1st and the 3rd floors	The Chi-Chi earthquake with PGA=200gal
Dam500_1F&3F	the 1st and the 3rd floors	The Chi-Chi earthquake with PGA=500gal
Dam1200_1F&3F	the 1st and the 3rd floors	The Chi-Chi earthquake with PGA=1200gal

4.2.1 Damage Location Using LVDT-Measured Data

For cases of single damage location and two damage locations, Fig. 10 presents two *SubFRFDI* values of LVDT-measured data for Dam100_1F and Dam500_1F&3F, respectively The results reveal that these cases are predicted correctly by the *SubFRFDI* of LVDT-measured data.

For the *CurveFRFDI* values of LVDT-measured data, Fig. 11 presents the cases of single damage location and two damage locations, Dam100_1F and Dam500_1F&3F, respectively. The damage locations of the two cases are also predicted correctly by the *CurveFRFDI* of LVDT-measured data. The comparisons of Fig. 10 with Fig. 11 also reveal that, if the number of damage location is unknown, *CurveFRFDI* has higher sensitivity to damage than *SubFRFDI*.

4.2.2 Damage Location Using DIC-Measured Data

Fig. 12 presents the *SubFRFDI* values for a single damage location case and two damage locations, Dam100_1F and Dam500_1F&3F, respectively, of DIC-measured data. For comparison, Fig. 13 shows the *CurveFRFDI* values of DIC-measured data for the same experimental examples in Fig. 11. The results also show that the *CurveFRFDI* has higher sensitivity to damage than *SubFRFDI* as compared Figs. 10-11 with

Figs. 12-13. The results further indicate that applying the proposed approach to locate single and multiple nonadjacent damages to building structures is feasible by using DIC-measured displacements.

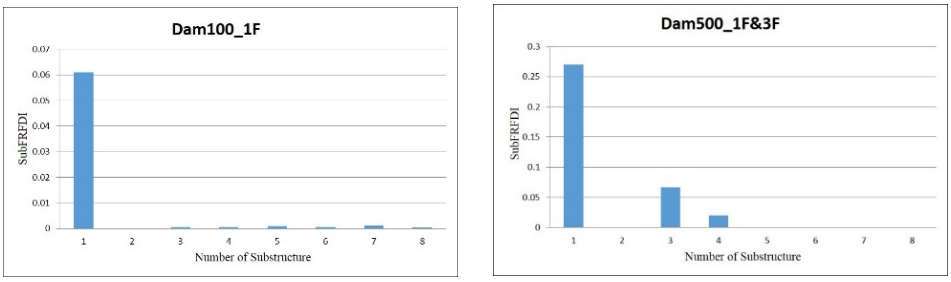

(a) (b)

Fig. 10 – *SubFRFDI* values of LVDT-measured data for (a) case Dam100_1F (b)

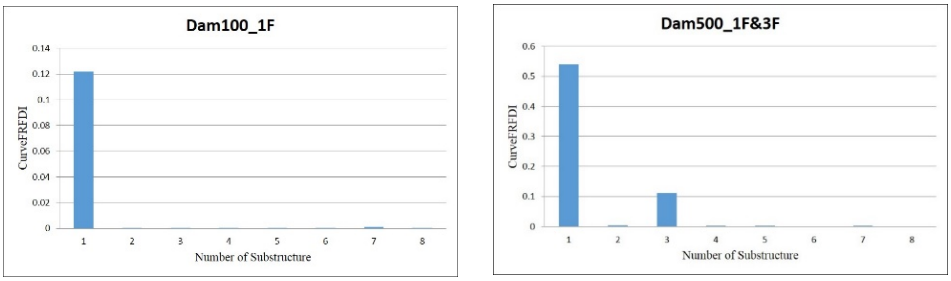

(a) (b)

Fig. 11 – *CurveFRFDI* values of LVDT-measured data for (a) case Dam100_1F (b) Dam500_1F&3F

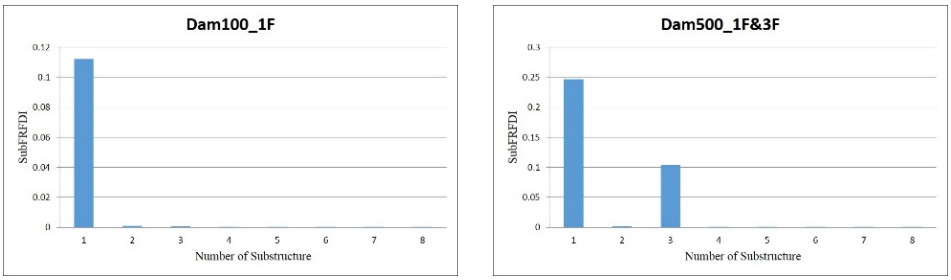

(a) (b)

Fig. 12 – *SubFRFDI* values of DIC-measured data for (a) case Dam100_1F (b) Dam500_1F&3F

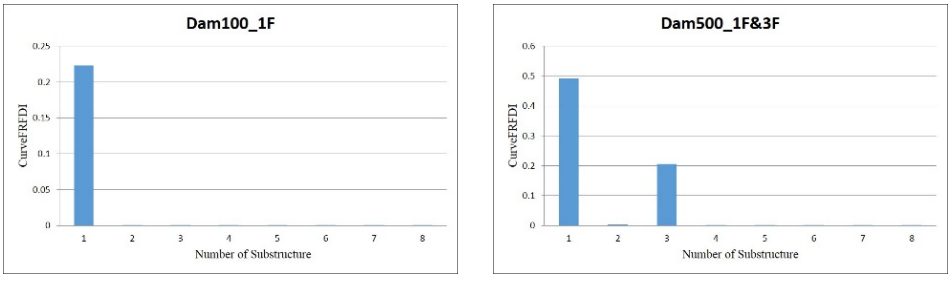

(a) (b)

Fig. 13 – *CurveFRFDI* values of DIC-measured data for (a) case Dam100_1F (b) Dam500_1F&3F

5. Conclusions

This work presents a displacement FRF-based approach for locating damage to building structures which enhance the work of Lin et al. [7]. Moreover, the feasibility of using DIC-measured displacement for the proposed approach to locate damage to building structures is investigated. A numerical example and an experimental example are presented to demonstrate the practicability of using the proposed approach to locate damage to shear-typed building structures. The following significant conclusions are drawn from the results herein.

1. Using *SubFRFDI* can predict damage location accurately for cases of single damage location. However, *SubFRFDI* is unable to locate damage for cases of multiple damage locations with large damage extent. Different from *SubFRFDI*, *CurveFRFDI* can locate damage no matter what its intensity (extent). Moreover, *CurveFRFDI* has higher sensitivity to damage than the *SubFRFDI*. Thus using *CurveFRFDI* can predict damage location more accurately than using *SubFRFDI* for cases of multiple damage locations with large damage extent.
2. For cases of multiple damage locations, some *CurveFRFDI* values corresponding to damaged locations may much smaller than others. To solve this drawback, a threshold *CurveFRFDI* value needs to be set to locate damage and the threshold *CurveFRFDI* value can be determined after numerous numerical simulations of damage scenarios for a certain building structure.
3. Applying the proposed approach and DIC-measured displacements to locate single and multiple nonadjacent damages to building structures is feasible. However, both *SubFRFDI* and *CurveFRFDI* are unable to locate damage for cases of multiple adjacent damage locations, it needs to be solved in future research.

4. Acknowledgements

The authors would like to thank the National Science Council of the Republic of China for financially supporting this research under Contract No. MOST 103-2625-M-009 -003 and MOST 104-2221-E-009 -049 -MY2.

6. References

[1] Carden EP, Fanning P (2004): Vibration based condition monitoring: A review. *Structural Health Monitoring*, **3**, 355–377.

[2] Fan W, Qiao P (2011): Vibration-based damage identification methods: a review and comparative study. *Structural Health Monitoring*, **10**, 83-111.

[3] Ni YQ, Zhou XT, Ko JM (2006): Experimental investigation of seismic damage identification using PCA-compressed frequency response functions and neural networks. *Journal of Sound and Vibration*, **290** (1-2), 242-263.

[4] Furukawa A, Otsuka H, Kiyono J (2006): Structural damage detection method using uncertain frequency response functions. *Computer-Aided Civil and Infrastructure Engineering*, **21** (4), 292-305.

[5] Kanwar VS, Kwatra N, Aggarwal P. Gambir ML (2008): Health monitoring of RCC building model experimentally and its analytical validation. *Engineering Computations*, **25** (7-8), 677-693.

[6] Hsu TY, Loh CH (2009): Damage detection using frequency response functions under ground excitation. *16th Int. SPIE Symp. on Smart Structures and Materials and Nondestructive Evaluation and Health Monitoring*, San Diego, CA, USA.

[7] Lin TK, Hung SL, Huang CS (2012): Detection of damage location using a novel substructure-based frequency response function approach with a wireless sensing system. *International Journal of structural Stability and Dynamics*, **12** (4), 1250029.

[8] Lee U, Shin J (2002): A frequency response function-based structural damage identification method. *Computers and Structures*, **80**, 117-132.

[9] Celebi M (2002): Seismic instrumentation of buildings (with emphasis on Federal buildings). *Tech. Rep. 0-7460-68170*, United States Geological Survey, Menlo Park, Calif, USA.

[10] Ribeiro D, Calçada R, Ferreira J, Martins T (2014): Non-contact measurement of dynamic displacement of railways bridges using an advanced video-based system. *Engineering Structures*, **75**, 164–80.

[11] Shih MH, Sung WP, Tung SH, Bacinskas D, Kaklauskas G (2011): Developing three-dimensional digital image correlation techniques to detect the surface smoothness of construction materials. *International Journal of Materials and Product Technology*, **42** (3-4), 234–246.

[12] Shih MH, Sung WP, Chen SC (2012): Application of digital image correlation technique to monitor dynamic response of building under earthquake excitation. *Advanced Science Letters*, **5**, 963–966.

[13] Combe G, Richefeu V (2013): Tracker: a particle image tracking (PIT) technique dedicated to nonsmooth motions involved in granular packings. *7th international conference on michromechanics of granular media, AIP*, Sydney, Australia.

[14] Sieffert Y, Vieux-Champagne F, Grange S, Garnier P, Duccini J, Daudeville L (2016): Full-field measurement with a digital image correlation analysis of a shake table test on a timber-framed structure filled with stones and earth. *Engineering Structures*, **123**, 451–72.

[15] Lu YC, Hung SL, Lin TH (2014): Integrating a Hive Triangle Pattern with Subpixel Analysis for Noncontact Measurement of Structural Dynamic Response by Using a Novel Image Processing Scheme. *The Scientific World Journal*. Article ID 375210.

[16] Hung SL, Lu YC (2017): Integrating a hive triangle pattern with sub-pixel analysis for measurement of structural dynamic response by using GPU computing. *2017 Congress on Advances in Structural Engineering and Mechanics (ASM17)*, Iisan (Seoul), Korea.

